Recoil Momentum Spectroscopy of Highly Charged Ion Collisions on Magneto-Optically Trapped Na

J. W. Turkstra,[1] R. Hoekstra,[1] S. Knoop,[1] D. Meyer,[1,*] R. Morgenstern,[1] and R. E. Olson[2]

[1]*Kernfysisch Versneller Instituut, Atomic Physics, Rijksuniversiteit Groningen, Zernikelaan 25, NL-9747 AA Groningen, The Netherlands*

[2]*Physics Department, University of Missouri–Rolla, Rolla, Missouri 65401*

(Received 6 February 2001; revised manuscript received 18 June 2001; published 31 August 2001)

We have used a cold ($T \ll 1$ mK), laser-cooled target of Na atoms confined in a magneto-optical trap to study electron capture processes during highly charged ion-sodium atom collisions at keV energies. Momentum distributions of target ions were determined by employing time-of-flight and position sensitive detection of the Na ions, produced during the collisions and extracted by a weak electric field. In this way impact parameter sensitive information about multielectron capture processes is obtained.

DOI: 10.1103/PhysRevLett.87.123202 PACS numbers: 34.70.+e, 32.80.Pj

Electron capture processes during keV collisions of highly charged ions with various atomic and molecular targets play an important role in man-made and in astrophysical plasmas. These processes not only strongly influence the charge state balance but also give rise to light emission. An example that recently attracted a lot of attention is the soft x-ray emission resulting from the interaction of multicharged solar wind ions with Earth-passing comets such as Hale-Bopp and Hyakutake [1–4]. The understanding and theoretical modeling of one-electron capture from one-electron targets (alkalis and atomic hydrogen) is rather well established, see, e.g., [5], although for multicharged ions experimental verifications as a function of impact parameter are hardly existent. The knowledge of one-, two-, and, in particular, many-electron transfer from multielectron atoms and molecules, which are, for example, the main constituents of the cometary tails, is basically lacking, notwithstanding the fact that a whole arsenal of experimental methods has been applied to study these processes.

Almost all methods are based on the detection of the charge-changed ion, or its emission of electrons and photons [6]. Since electrons are most often quasiresonantly captured into excited orbitals of highly charged ions, radiative and Auger processes follow the primary capture process. Therefore photon and electron spectroscopy and charge-state measurements of the projectile ions are generally just derivatives of the initial capture processes, see, e.g., [7,8]. Recoil ion momentum spectroscopy (RIMS) in which the charge state and momentum of the recoiling target are measured is the most direct method to study one- and many-electron capture processes as a function of the impact parameter; for reviews, see, e.g., [9–11]. Additionally with RIMS one circumvents the difficulty of preparing highly charged ion beams that are strongly collimated and have a sufficiently small energy spread to resolve structures in the (small angle) differential scattering cross sections and to distinguish various inelastic or superelastic processes. For electron capture by highly charged ions, taking place at large impact parameters, the corresponding requirements regarding the beam quality are especially stringent.

From the collision kinematics one finds that the recoil energies are small, much less than 100 meV; therefore also the initial energy spread of the target needs to be controlled. During the last years COLTRIMS (cold target RIMS) has been developed [10–15] employing effusive and especially supersonic jets of rare gases as cold targets.

In this paper we report on a new generation of cold targets for COLTRIMS experiments. The ultracold targets ($T \ll 1$ mK) are obtained by laser cooling and trapping in a magneto-optical trap (MOT) [16–18]. Such a target has distinct advantages. It is cooled in all three dimensions and it is much colder than supersonic jets. Important for applications in storage rings, the particle load on the vacuum system is very low and with small magnetic fields the target position can be moved. But even more important it gives access to a rich palette of target atoms. Particularly all alkali and earth alkaline atoms which are quasi-one- or two-electron targets can be used just as many other elements from the periodic table, for example, Cr and Yb.

As a proof of principle and to show the potential of the method we produced a magneto-optically trapped Na target consisting of about 10^6 atoms, captured from a background Na vapor pressure of $\sim 10^{-9}$ mbar in a $\leq 10^{-9}$ mbar residual gas pressure. Details on the experiment will be given elsewhere [19]. Briefly, the laser-cooled target was trapped in a magnetic field with a gradient of ~ 3 mT/cm, and three sets of counterpropagating laser beams with a diameter of 20 mm each, red detuned from the $3s\,^2S_{1/2}(F = 2) - 3p\,^2P_{3/2}(F = 3)$ resonance line by 10 MHz (total light intensity around 100 mW). An electro-optical modulator is used to produce a "repumping" laser beam in order to avoid buildup of population in the $F = 1$ hyperfine level of the Na ground state. The fluorescence from the MOT is observed with a CCD camera. It shows that the cloud of target atoms is confined to a spherical volume on the order of 5–10 mm^3. By switching the MOT off and

on with different time delays we find a target temperature of 300 μK, which is a standard value for a Na MOT [17].

Figure 1 shows a schematic diagram of our experimental arrangement. A multicharged ion beam extracted from our electron cyclotron resonance ion source is chopped and collimated to 1 mm diameter in front of the experiment and enters the MOT volume through another 1 mm diaphragm. The ions enter in the midplane between two anti-Helmholtz coils such that they do not cross magnetic field lines. Na recoil ions formed via electron capture are extracted from the MOT region by a homogeneous electric field, tunable between a few V/cm and a few hundred V/cm. Extraction takes place perpendicular to both the projectile beam and the symmetry axis of the anti-Helmholtz configuration to minimize ion deflection by magnetic fields. After passing a short drift region of, at the moment, only 8 cm the ions are detected on a multichannel plate in conjunction with a delay line anode for position sensitive detection (ROENTDEK).

Figure 2 shows a time-of-flight (TOF) spectrum of Na^{q+} ions, resulting from 3 keV/amu O^{6+} collisions on Na. We observe recoil charge states up to 4+. The TOF spectrum is dominated by singly charged recoils. This reflects the fact that the Na($3s$) electron is loosely bound and therefore can be captured at large impact parameters. The background in the spectrum is mainly due to Na_2^+ molecular ions, continuously formed via associative ionization [20] in the interaction of two excited Na($3p$) atoms within the MOT.

For each detected ion not only its flight time but also its arrival position is registered and stored in a list-mode file. These data are subsequently analyzed off-line and used to determine the recoil momenta in the x, y, and z directions. The Na_2^+ molecular ions mentioned above are produced nearly at rest. Their arrival position at the detector is used to fix the zero point, i.e., the position of the target. Since the target atoms are not polarized, the collision system is cylindrically symmetric around the beam axis implying that there is no dependence on the azimuthal angle. Therefore, only the momenta in longitudinal (p_{long}) and transverse (p_{trans}) directions to the ion beam are relevant.

The transverse momentum is a measure for the impact parameter. The longitudinal momentum is given by (in atomic units) [11]

$$p_{\text{long}} = \frac{Q}{v_p} - \frac{1}{2} n v_p \tag{1}$$

with Q the difference between the total binding energies before and after the reaction, v_p the velocity of the primary ion, and n the number of transferred electrons.

The obtained experimental momenta or energy gain values Q are compared with the results from classical trajectory Monte Carlo (CTMC) calculations using the many-electron code described previously [21]. For the C^{6+} + Na system, the nine electrons of the L and M shells of Na and the two nuclei were included in the 11-body calculations. Hartree-Fock electronic energies were used for the description of the two $2s$, six $2p$, and one $3s$ electrons of Na [22]. For each trajectory, the initial state of the Na atom (nucleus and electrons) was initialized such that its center-of-mass position and momentum were set to zero. After each single or multiple electron capture event, the x, y, and z momenta of the Na^{q+} recoil ion were recorded. Since the product electron capture states are not quantized within the CTMC method, it is necessary to incorporate this fact to describe the data. This was easily accomplished by using hydrogenic n, l binning procedures successfully developed for predicting line emission spectra [23]. After determining the n values

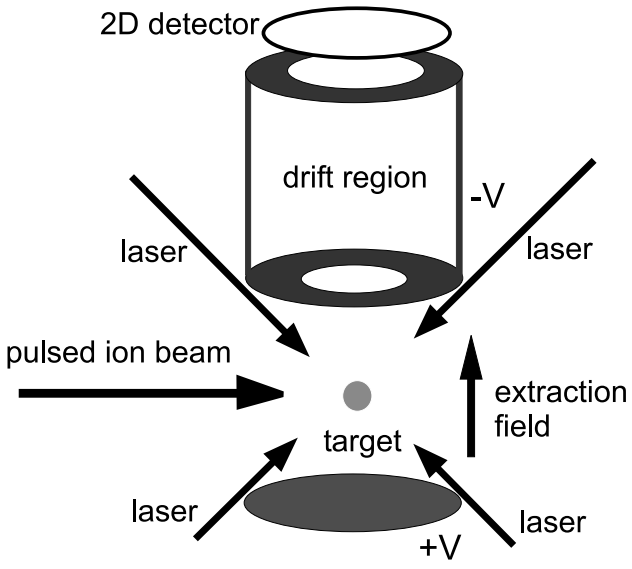

FIG. 1. Schematic representation of the apparatus. The third set of counterpropagating laser beams is perpendicular to the figure and enters the MOT along the symmetry axis of the coils (not shown) producing the anti-Helmholtz magnetic field configuration.

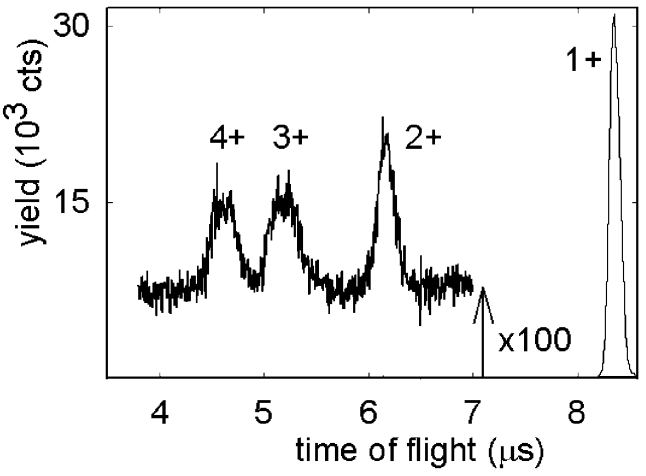

FIG. 2. Time-of-flight spectrum of 3 keV/amu O^{6+} ions colliding on Na. The peaks of the Na^{q+} recoils are labeled by their charge state.

of the captured electrons, the Q value for the reaction is uniquely given. The longitudinal momentum is related to the energy gain according to Eq. (1). As will be discussed, the binning procedure was applied to the single and double capture events only. For higher stages of multiple capture, the "classical" binding energies were used to calculate longitudinal momentum spectra. The transverse momentum spectra obtained from the CTMC method need not be modified by a subsequent binning procedure.

Figure 3 shows intensity plots, in which the number of detected Na^{q+} recoil ions is plotted as a function of p_{trans} and Q for $q = 1$, 2, 3, and 4. The overall trends in experiment and theory are similar. Na^{1+} ions are created with rather low transverse momenta. For Na^{2+} the momenta get larger, and for Na^{3+} and Na^{4+} they reach values up to 50 a.u. This reflects the fact that one-electron transfer takes place already at large impact parameters ($5 < b < 20$ a.u.), whereas for transfer of more electrons the relevant impact ranges are much smaller ($b \simeq 4$–5 for Na^{2+}, $b \simeq 3.5$–4.5 for Na^{3+}, and $b \leq 3.5$ for Na^{4+}). The negative values of Q correspond to negative values of p_{long}, implying that the target ions are recoiled into a direction opposite that of the outgoing projectile beam. This means that the collisions are "superelastic"; the transferred electrons are captured into more strongly bound states.

For a more quantitative comparison of the experimental data with the CTMC calculations we have integrated the data over either the energy gain or transverse momenta to obtain distributions of perpendicular momenta and energy gain spectra. For Na^{1+} and Na^{2+} recoil ions the projected distributions are shown in Fig. 4.

First considering only the transverse momenta, we find good agreement between CTMC and experimental distributions for Na^{1+}, Na^{2+}, and Na^{4+} (not shown). For Na^{3+} (not shown) the experimental distribution peaks around 30 whereas the CTMC has its maximum somewhat below 20. This indicates that as compared to theory smaller impact parameters contribute significantly to the three-electron removal processes. Since for Na^{4+} theory and experiment are in accordance with each other, it seems that three-electron transfer draws flux from the four-electron processes. This may be understood in an independent electron picture. In the four-electron channel, four electrons become molecular at short internuclear distance; at a certain point on the way out of the collision, when three electrons are transferred to the O^{6+} (reducing the projectile charge state to 3+), the fourth, least-bound electron may be recaptured by the now fourfold charged Na recoil ion. In the future, with improved experimental conditions we will investigate such interference effects between three- and four-electron processes in 2D plots as shown in Fig. 3.

Concerning the energy gain spectra we focus first on the Na^{2+} results. The CTMC calculations predict two channels to contribute, namely, true two-electron capture (labeled cc) and one-electron capture plus ionization (labeled ci). Both channels seem to describe the overall shape of the spectrum although relative intensities differ. Concerning the two-electron channel it is of note that the population of $O^{4+}(1s^2 3l 3l')$ and $O^{4+}(1s^2 3l 4l')$ states would correspond to Q values in the range of -51 to -37 and -34 to -24 eV, respectively. The $3lnl'$ states with $n \geq 5$ extend up to a Q value of 1 eV. These states are

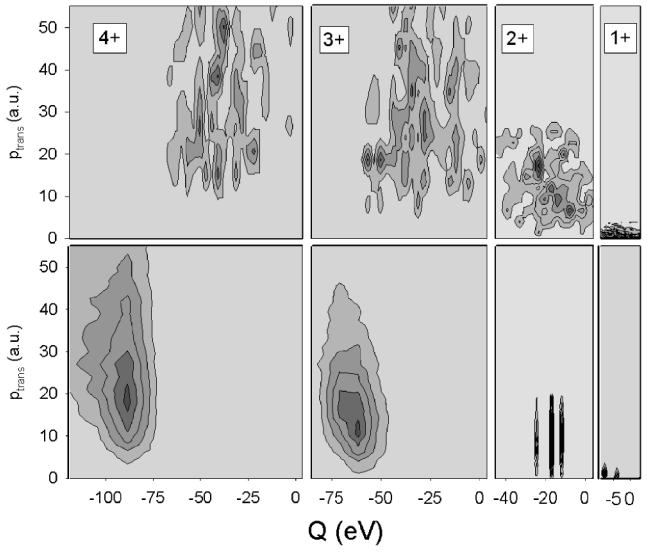

FIG. 3. Experimental (top row) and CTMC (bottom row) transverse momenta and energy gains of Na^{q+} ($q = 1$–4) recoil ions produced in 3 keV/amu O^{6+}-Na collisions.

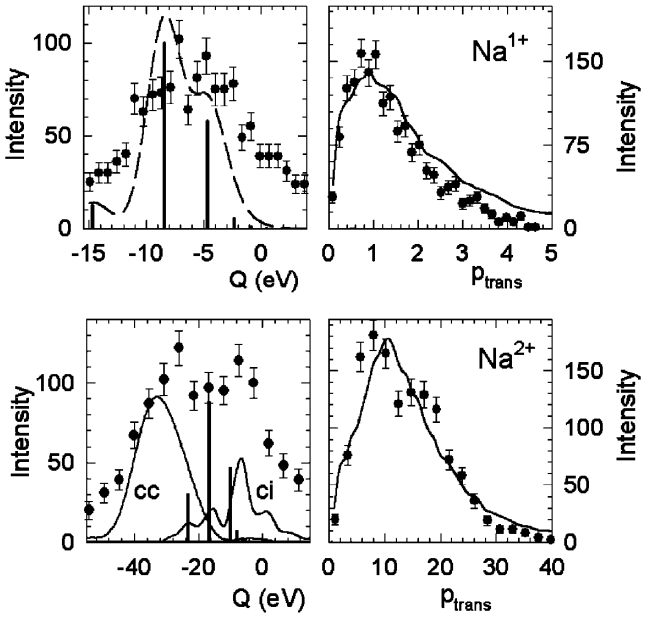

FIG. 4. Transverse momenta and energy gains of Na^{1+} and Na^{2+} recoil ions produced in 3 keV/amu O^{6+}-Na collisions. The CTMC results for C^{6+} are indicated by curves and bars (see text). For Na^{2+}, CTMC curves labeled cc and ci correspond to two-electron capture and one-electron capture plus ionization, respectively.

more strongly populated than expected from the classical CTMC distribution for two-electron capture.

Doing the hydrogenic binning of the CTMC results predicts these more asymmetric states to be populated. In Fig. 4 the three dominant bars correspond to $(3l, 4l')$, $(3l, 5l')$, and $(3l, 6l')$ configurations of C^{4+}. The configurations result from capturing the $3s$ and one of the $2p$ electrons of Na. In the classical independent electron description of the CTMC model, the $2p$ electron is transferred into a "classical state" which lies in the gap between the $n = 2$ and $n = 3$ principal quantum shells. The binning moves this electron up into the $n = 3$ shell. This is the main cause for the shift between the binned and unbinned CTMC results. In this respect the $3s$ electron plays only a minor part; because it is loosely bound, it ends up in higher lying orbitals which are close to a continuum of states. The large difference in binding energy of the $2p$ and the $3s$ electron validates the approach of two subsequent hydrogenic binning procedures, although it is clear that the final binding energy does not coincide with values for doubly excited states in O^{4+}. At lower energies where the ionization channels become small, the experiments will contribute to the understanding of independent versus correlated multielectron transfer.

The present experimental resolution can be seen from the Na^{1+} results. According to CTMC, capture into $n = 6$ and $n = 7$ dominates. The dashed curve in Fig. 4 shows the CTMC results folded with a Gaussian distribution corresponding to a momentum resolution of 0.25 a.u. The resolution is therefore $\sim 0.25-0.3$ a.u. This is not yet as good as or better than the record values of 0.07 a.u. obtained on He supersonic jet targets (cf. Dörner *et al.* [11] and references therein). However it is already similar to the resolution of heavier gas jet targets such as Ne and Ar. Presently our resolution is mainly determined by the short length of our time-of-flight drift region of only 8 cm [19]. The short drift length mandates extraction fields so low that contact potentials and Na coverages on the walls influence the field configuration. The setup will be upgraded with a drift region of about 50 cm and magnetic field supplies which will allow us to switch off the magnetic field during interaction and detection phases of the experiment opening up possibilities for laser aligning of target atoms.

Thus in this Letter we have illustrated the first use of a MOT trap for application to collision systems unavailable with conventional COLTRIMS experiments. It is now possible to investigate targets other than rare gases. Goals for the future are to improve the experimental resolution and to study the dynamics of collisions involving excited atomic targets.

We gratefully acknowledge the support of the KVI technical staff. As Project No. 99AQ03 this work is part of the research program of the Stichting voor Fundamenteel Onderzoek der Materie (FOM) which is financially supported by the "Stichting voor Nederlands Wetenschappelijk Onderzoek" (NWO). R. E. O. is supported by the Office of Fusion Energy Sciences, DOE, and NSF INT-9723737.

*Present address: Ruhr Universität, Bochum, Germany.

[1] C. M. Lisse *et al.,* Science **274**, 205 (1996).
[2] R. M. Häberli *et al.,* Science **276**, 939 (1997).
[3] V. A. Krasnapolsky *et al.,* Science **277**, 1488 (1997).
[4] P. Beiersdorfer, C. M. Lisse, R. E. Olson, G. V. Brown, and H. Chen, J. Appl. Phys. (to be published).
[5] W. Fritsch and C. D. Lin, Phys. Rep. **202**, 1 (1991).
[6] R. K. Janev and HP. Winter, Phys. Rep. **117**, 265 (1985).
[7] H. Cederquist *et al.,* Phys. Rev. A **61**, 022712 (2000).
[8] G. de Nijs, R. Hoekstra, and R. Morgenstern, J. Phys. B **29**, 6143 (1996).
[9] C. L. Cocke and R. E. Olson, Phys. Rep. **205**, 155 (1991).
[10] J. Ullrich *et al.,* J. Phys. B **30**, 2917 (1997).
[11] R. Dörner *et al.,* Phys. Rep. **330**, 95 (2000).
[12] R. Dörner, J. Ullrich, H. Schmidt-Böcking, and R. E. Olson, Phys. Rev. Lett. **63**, 147 (1989).
[13] V. Frohne *et al.,* Phys. Rev. Lett. **71**, 696 (1993).
[14] A. Cassimi *et al.,* Phys. Rev. Lett. **76**, 3679 (1996).
[15] A. A. Hasan, E. D. Emmons, G. Hinojosa, and R. Ali, Phys. Rev. Lett. **83**, 4522 (1999).
[16] E. L. Raab, M. Prentiss, A. Cable, S. Chu, and D. E. Pritchard, Phys. Rev. Lett. **23**, 2631 (1987).
[17] H. Metcalf and P. van der Straten, *Laser Cooling and Trapping* (Springer, Heidelberg, 1999).
[18] S. Wolf and H. Helm, Phys. Rev. A **56**, R4385 (1997).
[19] J. W. Turkstra, R. Hoekstra, S. Knoop, D. Meyer, R. Morgenstern, and R. E. Olson (to be published).
[20] H. A. J. Meijer, H. P. v. d. Meulen, and R. Morgenstern, Z. Phys. D **5**, 299 (1987).
[21] R. E. Olson, J. Ullrich, and H. Schmidt-Böcking, Phys. Rev. A **39**, 5572 (1989).
[22] C. F. Fischer, *The Hartree-Fock Method for Atoms* (John Wiley Publishing, New York, 1977).
[23] R. Hoekstra *et al.,* J. Phys. B **26**, 2029 (1993).